Synthesis and Ex-situ Characterization of Nafion/TiO_2 Composite Membranes for Direct Ethanol Fuel Cell

Lepakshi Barbora,[1] *Simadri Acharya,*[2] *Anil Verma**[2]

Summary: Nafion/TiO_2 composite membranes for different loadings of TiO_2 were prepared by casting method for the possible application in direct ethanol fuel cell (DEFC). The properties of the composite membranes were investigated by scanning electron microscopy (SEM), x-ray diffraction (XRD), thermogravimetric analyser (TGA), ion exchange capacity, water and alcohol uptake, swelling ratio, proton conductivity, and ethanol crossover. The observed characteristics of the membranes were evaluated for DEFC and compared with the direct methanol fuel cell (DMFC) membrane. The analysis reveales a significant influence on the TiO_2 surface characteristics, water and alcohol uptake, and swelling of the membrane. The TiO_2 composite membranes exhibited a sharp decrease in methanol and ethanol crossover for 5% TiO_2 and the proton conductivity was heighest for 1% TiO_2 loading. The best compromise between proton conductivity and crossover has been found out with the help of the characteristic factor ϕ. The optimum loading of 5% TiO_2 composite membrane has shown the maximum characteristic factor.

Keywords: composite; crossover; direct ethanol fuel cell; morphology; nafion

Introduction

Polymer electrolyte membrane fuel cells with liquid-feed offer a promising alternative to hydrogen gas consuming fuel cell as they allow easy handling and storage of the liquid fuel for applications in portable and mobile electronic devices.[1] Many liquid fuels such as methanol,[2] ethanol,[3] formic acid,[4] ethylene glycol[5] are being tested as a fuel in polymer electrolyte membrane (PEM) based fuel cell. Among all the investigated possible fuels, methanol[6,7] is the most favorite due to its relatively higher electrochemical activity, which is one of the major prerequisites for PEM based fuel cell. The fuel cell, which utilizes methanol as a fuel is known as direct methanol fuel cell (DMFC) and has been actively investigated since 1960s.[8] Much progress has been made in the different relevant issues of DMFC, including electrocatalysts, electrolyte, membrane electrode assembly and fuel cell stack. However, the sluggish anode kinetics and methanol crossover (undesired permeation through the membrane) are still the main challenges to the commercialization of direct methanol fuel cell despite that extensive efforts have been devoted.[9] Moreover, methanol is toxic and it is neither a primary nor a renewable fuel.[10] On the other hand, ethanol as a renewable material, offers an attractive alternative as a fuel in PEM based fuel cells with positive impact on both economy and environment.[11] Ethanol can be produced in large quantities from agricultural products and it is the major renewable biofuel from the fermentation of biomass. It should also

[1] Centre for Energy, Indian Institute of Technology Guwahati, Guwahati, Assam-781039, India
[2] Department of Chemical Engineering, Indian Institute of Technology Guwahati, Guwahati, Assam-781039, India
Fax: +91 361-2582291;
E-mail: anil.verma@iitg.ernet.in

be noted that ethanol and the intermediate products of ethanol electro-oxidation are less toxic than the methanol.[12] Therefore, the research on ethanol based fuel cell, direct ethanol fuel cell (DEFC), has become one of the promising fields of investigation. The research and development of DEFC have been concentrated on both the ethanol electro-oxidation mechanism[13] and identification of ethanol oxidation products over electro-catalysts.[14] Breaking the C–C bond in ethanol molecule for its complete electro-oxidation to CO_2 is a major problem in ethanol electrocatalysis. It was shown that the main bulk products in the electrochemical oxidation of ethanol were acetaldehyde, acetic acid, and CO_2.[15] In particular, acetic acid causes a considerable lowering of the fuel capacity to generate electricity and yield environmental problems. Therefore, it is important to develop highly selective catalysts for complete oxidation of ethanol to carbon dioxide to enhance the electrochemical reaction rate.[11] Antolini (2007)[16] presented an overview of the catalysts tested as anode and cathode materials for DEFC.

Although the research and development work on DEFC are being done but the investigation on the problem of ethanol crossover in DEFC similar to methanol crossover in DMFC is scanty. When the ethanol is fed to the anode side of the fuel cell, some of the ethanol permeates through the polymer electrolyte membrane to the cathode (known as crossover). Song et al. (2005)[8] investigated the behavior of methanol and ethanol permeation through Nafion-115 and its effect on the performance of fuel cell. They have shown that ethanol has lower permeability as compared to methanol inspite of the higher swelling ratio of nafion membrane in ethanol solution. It was found that methanol and ethanol permeability rates in the fuel cell increased with the increase in temperature and alcohol concentration. Fuel crossover through the PEM adversely affects the performance of the fuel cell, which requires the modification of existing membrane properties or the development of new membrane. In the effort of modifying the existing membrane properties, incorporation of inorganic additives are being investigated with the objective of serving the dual functions of improving water retention as well as providing more tortuosity to reduce the fuel crossover through the membrane. Blasi et al. (2006)[16] fabricated composite nafion membrane with nafion ionomer and silica to investigate the behaviour of the composite membrane for DEFC application. They observed that the increased water retention characteristics of these composite membranes did not enhance the fuel cell performance at temperatures below 90 °C and larger ethanol permeability was envisaged. Tan et al. (2006)[18] investigated the performance of nanocomposite membranes based on sulfonated poly(etheretherketone) and poly (ether sulfone), structured with silica modified by phosphotungustic acid for direct ethanol fuel cell. The composite membrane showed increased proton conductivity and mechanical stability, while the swelling in ethanol solution was reduced. Although the modified membranes showed a slight increase in ethanol permeability the other positive contributions, especially the increase in proton conductivity renders composite membrane suitable for DEFC application. Affoune et al. (2005)[19] studied the effect of methanol, ethanol, 2-proponol and water on the proton conductivity and surface properties of nafion membrane. They have established that both conductivity and surface topology of nafion undergo high modification when the membrane was transferred from water to alcohol environment. Arico et al. (1998)[14] conducted fuel cell experiments with methanol or ethanol as fuel and found that the ethanol permeability is less as compared to methanol permeability. The reduction of fuel permeability is important but at the same time the proton conductivity of the composite membrane must not be reduced. There is lack of extensive study in the field of composite membrane for the DEFC.

In the present study, nafion/TiO_2 composite membrane is synthesized and extensive ex-situ characterization of the composite membrane is conducted for the possible use in DEFC. Different loadings of TiO_2 have been used to prepare the composite nafion membrane. The membranes have been characterized for surface morphology, crystallinity, thermal stability, ion exchange capacity, water and alcohol uptake, swelling ratio, proton conductivity and ethanol permeability.

Experimental Part

Materials

Nafion® dispersion (SE-5112), 5wt% solid, was procured from DuPont, USA. Dimethylformamide (DMF) was purchased from Merck, India. Titanium dioxide (TiO_2, anatase) was obtained from Merck, Germany. Methnaol and ethanol were procured from Merck, India. All the chemicals were used without further purification and de-ionized water was used in all the experiments.

Method

Preparation of Membrane

The nafion dispersion had water and isopropyl alcohol as the major volatile constituents. The dispersion was dried to obtain dried solid residue of the nafion polymer. The dried solid nafion was dissolved and diluted in an appropriate amount of DMF as a solvent to get nafion solution. Membrane was prepared using solution casting method at 160 °C from the above obtained nafion solution.[20] The membrane thus prepared in the process was pure cast nafion membrane.

To prepare the composite nafion membrane, TiO_2 powder was calcined at 400 °C in a muffle furnace. A known amount of TiO_2 powder was added into the nafion solution and sonicated in an ultrasonic water bath (Model: D-78224, Make: Elma) to get fine dispersion of TiO_2 in the nafion solution. The dispersion was then used to cast the composite nafion membrane. The membranes before characterization were treated by boiling in 3% H_2O_2 to remove trace organics and then the sulphonic side chains were converted to the acid form (SO_3H^+) by boiling in 1M H_2SO_4.[20] Excess H_2SO_4 was removed from the membrane by rinsing in boiling water for 2 h followed by water rinsing to remove any remaining free acid. The membrane was stored in 18 MΩ water. All the properties of the membrane were evaluated at 25 °C. TiO_2 loading is reported in terms of weight percentage unless otherwise stated.

Membrane Characterization

SEM, TGA and XRD

Membrane thickness was measured by using scanning electron microscope (SEM) at several cross-sections of the sample. SEM was utilized for the surface morphology of TiO_2 powder, distribution of TiO_2 particles in the membrane and the interface between nafion and TiO_2 in the composite membrane.

Thermal stability of the membrane was investigated by using thermo gravimetric analyzer (TGA) (Mettler Toledo TGA/STDA 851) with a heating rate of 10 °C per minute in nitrogen atmosphere from 25 to 800 °C.

X-ray diffraction (XRD) measurements were carried out by using Bruker AXS-D8 Advance X-ray diffractometer using a Cu-Kα source operated at 40 keV and at a scan rate of 0.05 °/S.

Ion Exchange Capacity

The ion exchange capacity of the membrane was determined by titration method. The membrane was immersed in 0.1N NaOH solution for 24 hours under continuous stirring. To assure complete ion exchange, the samples were immersed again in another 0.1N NaOH solution for additional 24 hours. In the process, the H^+ sites of the nafion were explained by Na^+ through immersion of the membrane in the NaOH solutions. The two solutions were mixed for the accurate results and a sample was taken from the mixture. The

sample was titrated for displaced H^+ ions present in the sample using 0.1N HCl solution using phenolphthalein as an indicator. The ion exchange capacity of the membrane, E (meq/g), was calculated using eq. (1),[22,23]

$$\mathrm{E(meq/g)} = \frac{(V_{\mathrm{NaOH}}N_{\mathrm{NaOH}} - V_{\mathrm{HCl}}N_{\mathrm{HCl}})}{W_{\mathrm{d}}} \quad (1)$$

where, V_{NaOH} and V_{HCl} are the volumes (in ml) of NaOH and HCl solutions used in the titration, respectively. N_{NaOH} and N_{HCl} are the normalities of NaOH and HCl solutions, respectively. W_{d} is the weight of the dry membrane in gram.

Water and Alcohol Uptake

The water uptake of the membrane was measured by suspending a dry membrane sample of known weight in de-ionized water for 24 hours. Thereafter, the membrane was removed from water and the excess surface water was quickly wiped by tissue paper from both the surfaces to get the wet swollen membrane. The weight of the wet membrane sample was measured. Water uptake of the membrane was calculated by the following equation, eq. (2),

$$\mathit{Water\ uptake} = \frac{(W_{\mathrm{w}} - W_{\mathrm{d}}) \times 100}{W_{\mathrm{d}}} \quad (2)$$

where, W_{w} and W_{d} are the weights of wet and dry membranes, respectively.

Swelling Ratio

The swelling ratio of the membrane was determined by measuring the change of the membrane geometrical area (at a constant thickness of 80 μm) upon equilibrating the membranes in water or methanol or ethanol at room temperature. The swelling ratio was calculated using eq. (3),

$$\mathit{Swelling\ ratio}(\%) = \frac{(A_{\mathrm{w}} - A_{\mathrm{d}}) \times 100}{A_{\mathrm{d}}} \quad (3)$$

where, A_{w} and A_{d} are the area of wet and dry membranes, respectively.

To reduce the error, the measurements were repeated at least five times for each sample and arithmetic mean was used to report the data. The variations in the experimental values were in the range of ±5%.

Proton Conductivity

Normal direction conductivity of the membrane was determined in a conductivity cell shown in Figure 1. The conductivity measurement was performed in a two-electrode AC impedance mode using LCR meter. The membrane was fixed between flanges of the two compartments of the conductivity cell. The two platinum foil electrodes (0.5 cm^2) were placed near the faces of the membrane.

Conductivity measurements were performed at 25 °C after equilibrating the membrane in de-ionized water for 24 hours. The membrane was located at the center of the two chambers filled with 0.5 M H_2SO_4 solution in the conductivity cell. The electrical resistance of membrane (R_1) was measured at a frequency of 10 kHz and a voltage of 1V using LCR meter (HP, Model: 4263B). The electrical resistance of 0.5 M H_2SO_4 solution (R_2) without a membrane was also measured. The electrical resistance, R, of the membrane was calculated by subtracting the value of R_2 from R_1.

The conductivity of the membrane, σ (S/cm), was calculated using eq. (4),[24]

$$\sigma = \frac{L}{RA} \quad (4)$$

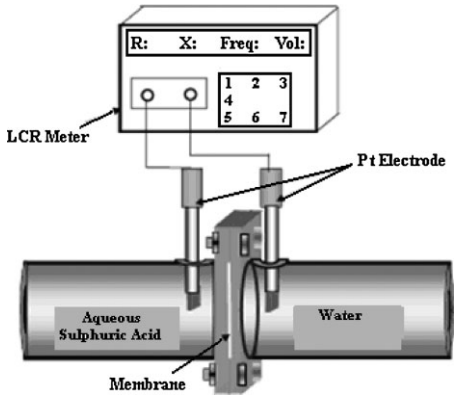

Figure 1.
Schematic diagram of the experimental set-up to measure proton conductivity.

where L, R, and A denote the distance between the electrodes (cm), the measured resistance (ohm), and the effective area of the membrane (cm^2) perpendicular to ion flow, respectively.

Ethanol Crossover

Ethanol crossover of the membrane was investigated in terms of the permeability of the ethanol through the membrane in a permeability test set-up.[24] The membrane to be tested was placed between the flanges separating the two chambers of the ethanol permeability cell. One chamber of the cell was filled with ethanol solution, while the other one with pure water. The crossed over ethanol concentration with time in the water compartment was determined by gas chromatograph (Varian CP-3800). After measuring the change in ethanol concentration with permeation time, the ethanol permeability (P) in cm^2/s through the membrane was obtained using the following relationship eq. (5),[25]

$$C_B = \frac{APC_A t}{V_B L} \quad (5)$$

In the above equation, C_A is the initial ethanol concentration (M) and C_B is the ethanol concentration (M) in the water compartment at time t in sec. V_B represents the volume of pure water (cm^3) and L the thickness of the membrane (cm), and A the area (cm^2) of the membrane.

Results and Discussion

Membrane characterization

SEM, TGA and XRD

Figure 2a to 2f shows the SEM images of pure cast nafion and composite nafion membranes at different loadings of TiO_2. It can be seen that all the membranes are dense and there is no evidence of pores or cracks. The TiO_2 particles are well dispersed in the membranes with 1%, 3% and 5% loadings (Figure 2b, 2c and 2d). The dispersion of TiO_2 in case of 7% and 9% loadings (Figures 2d and 2e) is somewhat not well dispersed and shows the aggelomeration in the composite membrane.

The thickness of the membrane was evaluated from the cross-sectional SEM images and found to be 80 μm with maximum 10% error.

Figure 3 shows the thermal stability results of pure cast and composite nafion membrane. On comparison of the TGA thermograms of the composite membranes with pure cast nafion membrane (Figure 3), it is observed that all the membranes retain more than 90% of its weight up to a temperature of about 310 °C. Above 310 °C, the composite membranes started to decompose and lost weight quite rapidly. This decomposition behavior below 300 °C can be attributed to the loss of bound and unbound water and rapid weight loss at and above 310 °C may be because of loosening of sulfonic acid groups present in the membrane.[26] The degradation of the composite membrane is very slow above 500 °C and the residue remaining is proportional to the TiO_2 content. The nafion/TiO_2 composite membranes showed not much improvement in thermal degradation temperature as compared with pure cast nafion but it is well beyond the desirable fuel cell operation temperature (25–80 °C).

The typical XRD patterns of TiO_2 powder, and the composite membranes at different TiO_2 loadings are represented in Figure 4(i) and 4(ii), respectively. The peaks observed for TiO_2 and nafion are almost identical to those reported in the literature.[26] The crystallite size of the TiO_2 powders are determined with the Debye-Scherrer equation using full-width at half maximum of the main diffraction peak and found to be about 16 nm. The patterns of composite membrane show the characteristic peak of the inorganic additive (TiO_2) indicating the presence of crystallites in the composite membranes. On comparing the XRD patterns, it can be concluded that the crystallinity of the composite membrane increased with the addition of 5% and 7% titanium dioxide. Addition of crystalline domains into the otherwise amorphous nafion membranes is expected

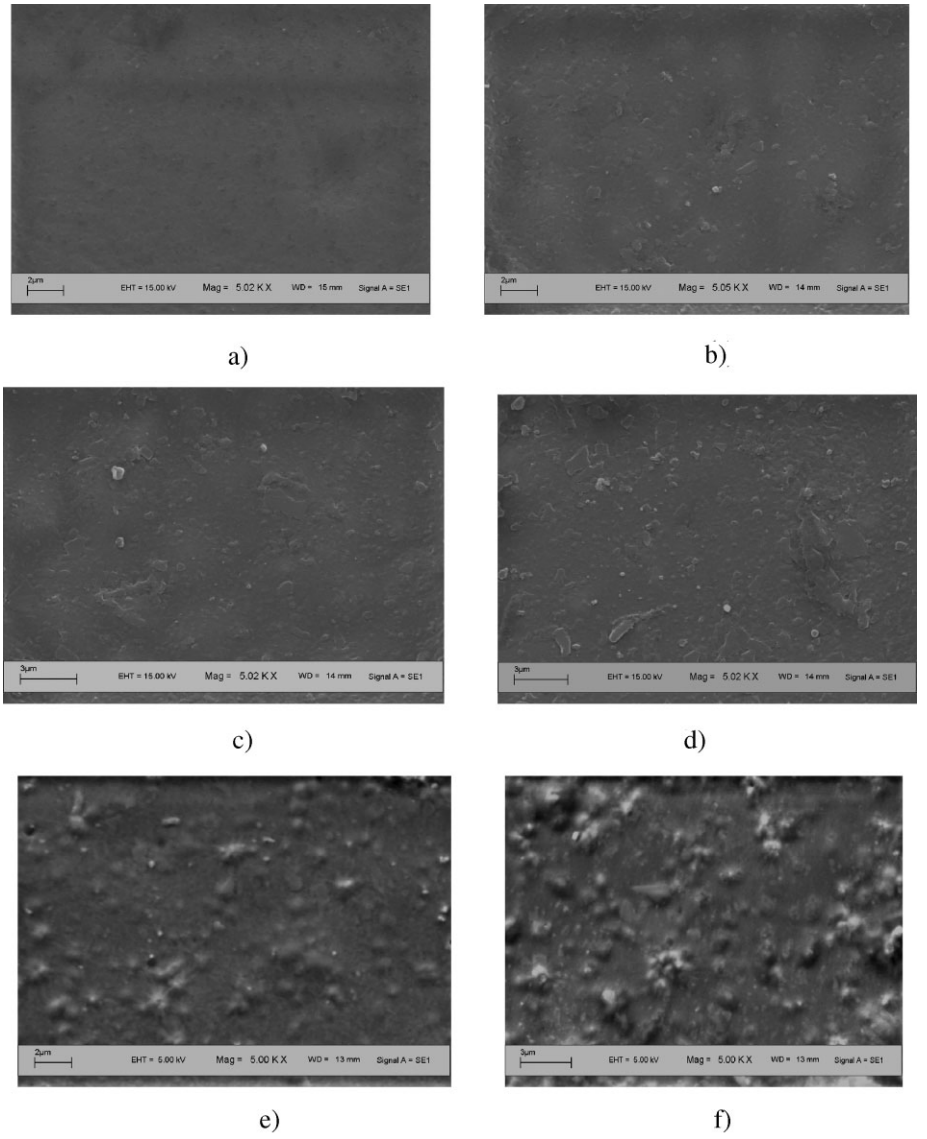

Figure 2.
SEM images of (a) Pure cast Nafion membrane (b) 1% Nafion/TiO_2 composite membrane (c) 3% Nafion/TiO_2 composite membrane (d) 5% Nafion/TiO_2 composite membrane (e) 7% Nafion/TiO_2 composite membrane and (f) 9% Nafion/TiO_2 composite membrane.

to decrease the fuel permeability, as crystalline surfaces are less permeable to liquid compared to amorphous surfaces.

Ion Exchange Capacity

Ion exchange capacity (IEC) is the number of replaceable ions (H^+) per unit mass of the dry membrane. This is one of the very important characteristics of the membrane as it provides an indication of the acid groups having H^+ ions. These H^+ ions are relatively weakly attached to SO_3^- groups and are able to move from anode to cathode via the Grotthuss mechanism.[28] This

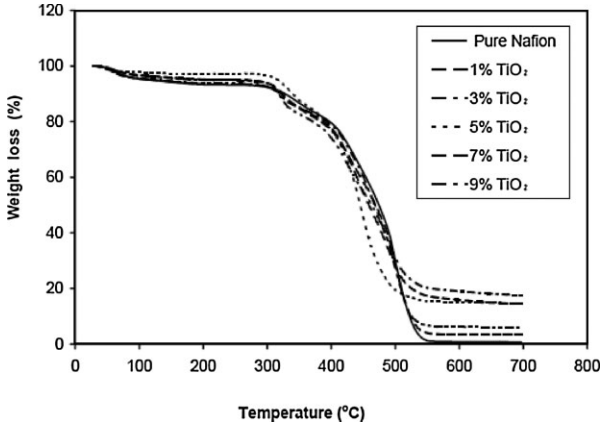

Figure 3.
TGA curves of pure and composite nafion membranes at different TiO_2 loading

mechanism involves very rapid 'hopping' of protons between neighboring sites involving solvated H^+ ions. Figure 5 shows that the IEC of the composite nafion membrane increases with 1% TiO_2 loading but on further increase in TiO_2 loading the IEC decreases slowly. The increase in the IEC for composite membrane is attributed to the TiO_2 particles. The strong oxidation potential of TiO_2 oxidizes the water molecules associated to it, which results in the formation of Ti-OH groups on the surface of the particles.[29] These additional OH groups increase the number of ion exchange sites in the composite membranes. These hydroxyl groups coordinate with the significant number of water molecules and thus increase the water content inside the composite membranes. The increased amount of water helps to loose the interaction between proton and SO_3^- ion. Thus more number of replaceable protons are available and measured by ion exchange capacity. It can be confirmed from Figure 6, in which the ion exchange capacity follows the pattern of water content in the membrane. The water content in the composite membranes is described in the subsequent section.

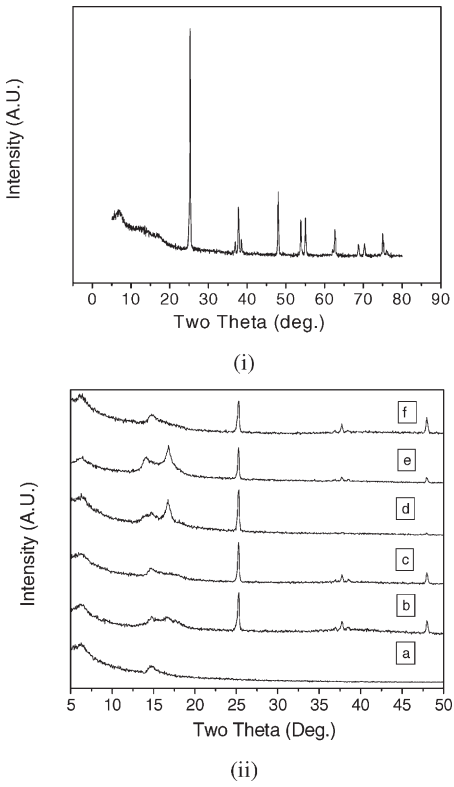

Figure 4.
XRD patterns of (i) TiO_2 powder, and (ii) composite membranes at different TiO_2 loadings (a) 0% (b) 1% (c) 3% (d) 5% (e) 7% (f) 9%.

Water and Alcohol Uptake

Water uptake is closely related to the basic membrane properties and plays an essential role in the membrane behavior. Proton conductivity and fuel permeation across the membrane depend to a large extent on the amount of water absorbed by the membrane. Presence of water in the membrane

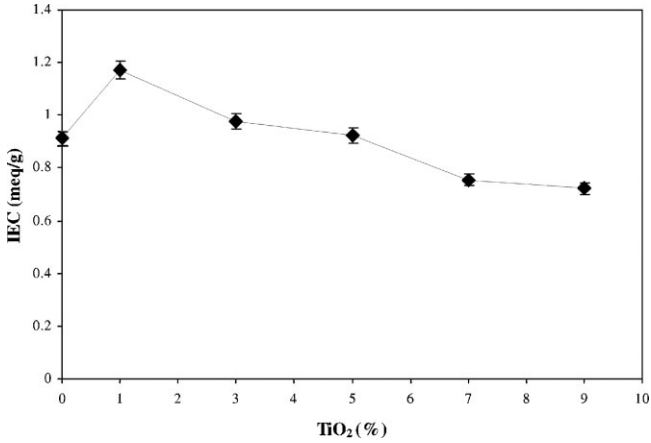

Figure 5.
Effect of TiO_2 content on IEC.

influences the ionomer microstructure, cluster, channel size, plasticizes and modifies the mechanical properties.[30] Water uptake properties of the composite membranes and pure cast nafion membrane were evaluated with de-ionized water. Figure 6 shows the percentage of water and alcohol uptake with TiO_2 loadings. Nafion/TiO_2 composite membranes have higher water and alcohol uptake than pure cast nafion membrane. The enhanced water uptake can be attributed to the hygroscopic nature of TiO_2.[31] A significant number of water molecules can be coordinated by hydrogen bonding with the OH groups present on the surface of TiO_2 particles.[28] Therefore, the water uptake of the composite membrane increases with the addition of the TiO_2 in the membrane till 1%. On further increase in TiO_2 loading to 5% the water uptake decreases but at any time the water uptake is more than the pure cast nafion membrane. But the composite membranes with TiO_2 loadings in the range of 7% to 9% showed water uptake lower than the pure cast nafion membrane. This may be attributed to the distribution of TiO_2 and the availability of active sites (OH

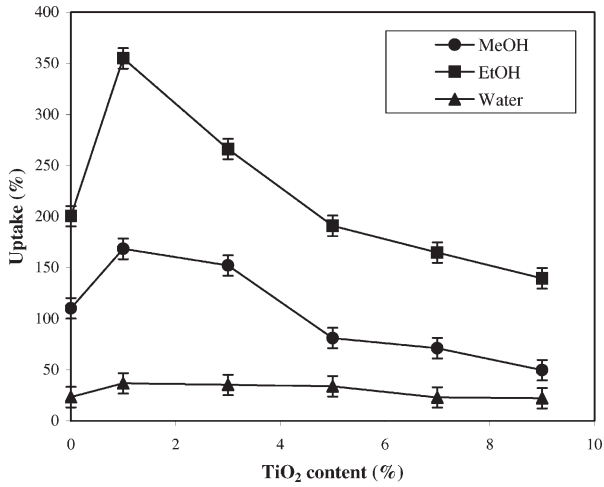

Figure 6.
Effect of TiO_2 content on water and alcohol uptake.

attached with TiO_2) on the surface of the composite membrane for hydrogen bonding with water. As can be seen from the SEM images (Figures 2b–2f), with increase in TiO_2 loading by 7% in the composite membranes, the formation of lump increased and the surface area of the TiO_2 increase. Over and above non-hydrogen bonding between OH groups of adjacent Ti-OH may be responsible for the decrease of free OH groups on the composite surface for hydrogen bonding with water.

Nafion has both hydrophobic and hydrophilic domains. Water being the most polar has high accessibility to the hydrophilic domains, which covers about 25 to 35% of the membrane mass as is obvious from the water uptake results. Hence, the membranes show lowest uptake for water. Methanol being less polar than water has accessibility to both the hydrophilic and hydrophobic domain whereas ethanol being the least polar will have maximum access to the hydrophobic domain (about 65 to 75% of the membrane mass) and to some extend to the hydrophilic domain as well. Hence, the uptake of ethanol is highest followed by methanol and water.

Figure 7 shows the uptake of three different concentrations of methanol and ethanol. The uptake increases with increase in concentration of methanol or ethanol, but in case of methanol the difference is less compared to ethanol, which again may be attributed to its polarity compared to ethanol.[32]

Swelling Ratio

Swelling is one of the important characteristics of the fuel cell membrane as it is sandwiched between two electrodes in the fuel cell. The electrodes and membrane form membrane electrode assembly (MEA), which is the vital part of the fuel cell. In a fuel cell on/off cycles the MEA gets wet and dry and may create cracks or delamination of electrodes in the MEA. Thus more permeability of the fuel will take place and the fuel cell performance will be reduced. Therefore, there should be a balance between the water uptake (a desired property) and the swelling (an undesired property). Figure 8 shows the trend of swelling ratio with the change in TiO_2 loading in the membrane. Swelling ratio follows the trend of water or alcohol uptake.

Proton Conductivity

For a hydrous polymer membrane to be a good proton conductor, it should have the presence of fixed charged sites surrounded by the water molecules, which facilitate the

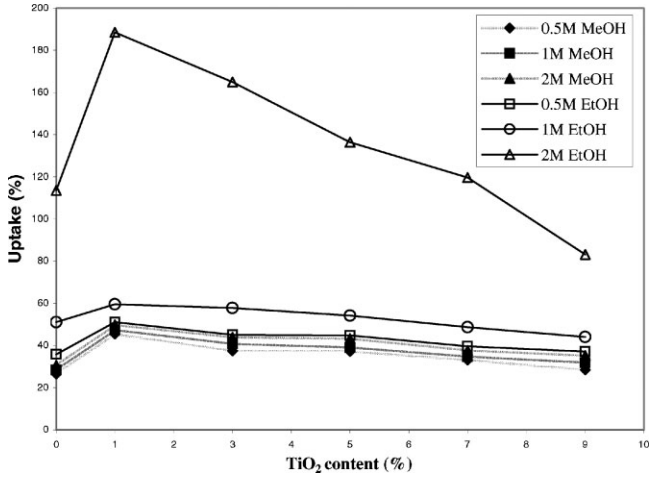

Figure 7.
Effect of TiO_2 content on uptake of alcohol of different concentrations.

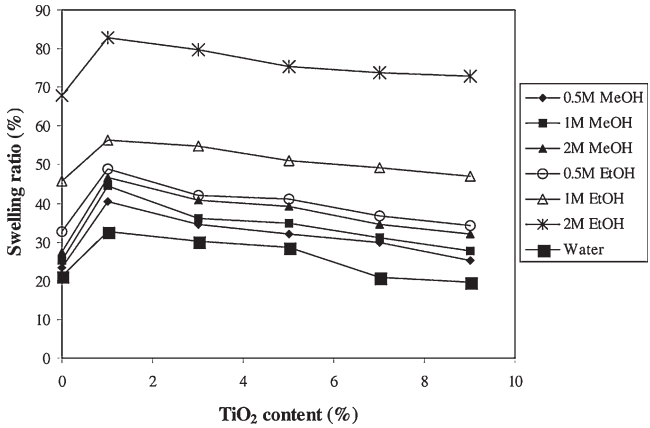

Figure 8.
Effect of TiO_2 content on membrane swelling.

transport of protons. The hydrogen ions (protons) are attached to the fixed sulphonic acid sites pending with the polymer chain. The protons conduct in the polymer by the hopping mechanism as described earlier. The replaceable characteristic of the ion has been discussed in terms of the ion exchange capacity. The fixed charged (SO_3^-) sites provide the centers where the moving ions (protons) can be accepted or released. In a polymer structure, maximizing the concentration of these charged sites is critical to ensure high conductivity. However, excessive addition of ionically charged side chains may significantly decrease the mechanical stability of the polymer, making it unsuitable for the fuel cell use. As discussed earlier that TiO_2 may change the morphology of the membrane by changing the shape of the ionic cluster and water content. Therefore, the proton conductivity is measured for the composite membrane with different loading of TiO_2.

Figure 9 shows that proton conductivity of composite membrane increased for 1% loading of TiO_2. On further increase in TiO_2 content the conductivity decreases slightly. The increase in proton conductivity is because of the increase in ion exchange capacity and water content of the composite membrane, which facilitates the transfer of protons. The decrease in proton

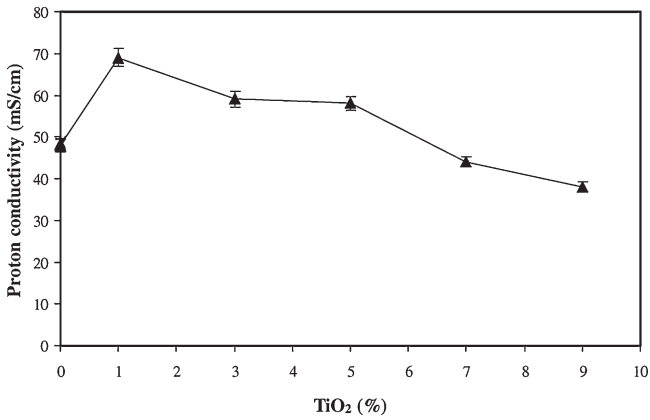

Figure 9.
Effect of TiO_2 content on proton conductivity.

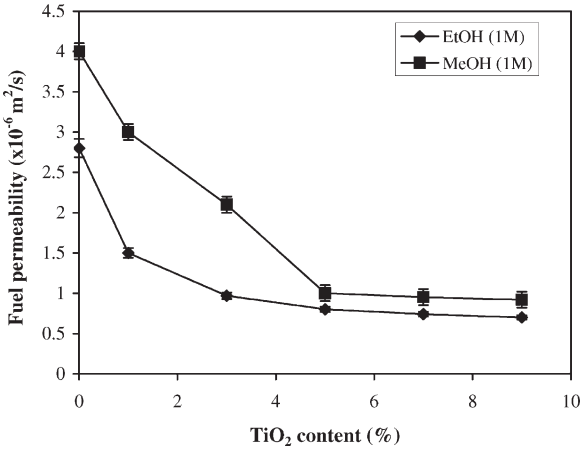

Figure 10.
Effect of TiO_2 content on fuel permeability.

conductivity with the increase in TiO_2 content may be attributed to a blocking effect by TiO_2 particles, which disrupt the continuum of sulfonic group clusters that are responsible for the proton motion in the nafion structure.[33]

Ethanol Crossover

The permeability of ethanol has been investigated for 1M concentration and compared with the methanol permeability through the membranes. Figure 10 shows that methanol and ethanol permeability of composite membranes is reduced as compared to pure cast nafion membrane. Fuel permeability through the composite membrane decreases with an increase in the TiO_2 loading. Thus, pure cast nafion membranes are more permeable than nafion/TiO_2 composite membranes of the same thickness. From the alcohol uptake results it was expected that ethanol would give a higher fuel permeability compared to methanol. But the experiment results showed that methanol permeability was higher than ethanol. This may be attributed to the difference in the geometry of the molecules and also to the coupling effect between ethanol and water molecules, which influences the independent transport of ethanol and water molecules through nafion membrane.[34]

The 5% TiO_2 loading decreases the permeability of the membrane for ethanol and methanol by 71% and 75% respectively. Further increase in TiO_2 loading by 7% and 9% do not show significant improvement in reduction of permeation. However, it is known that the polymer electrolyte membrane for direct alcohol fuel cell (DAFC) application should have the lowest fuel permeability and highest proton conductivity possible.[22] Thus, a relationship between the permeability and proton conductivity is an important factor in evaluating membrane performance for DAFC. This relationship is expressed as the characteristic factor[35], ϕ, calculated by using eq. (6),

$$\phi = \frac{\sigma}{P} \tag{6}$$

where, σ is the proton conductivity (mS/cm) and P is the fuel permeability (cm^2/s) of the membrane. Figure 11 shows the variation of characteristic factor of the membranes. The characteristic factor increases with the increase in TiO_2 content upto 5%. The high ϕ values are attributed to the sharp decrease in fuel permeability relative to a moderate increase in proton conductivity. The high ϕ values of composite membranes indicate that the nafion/TiO_2 composite membranes developed may be efficient for

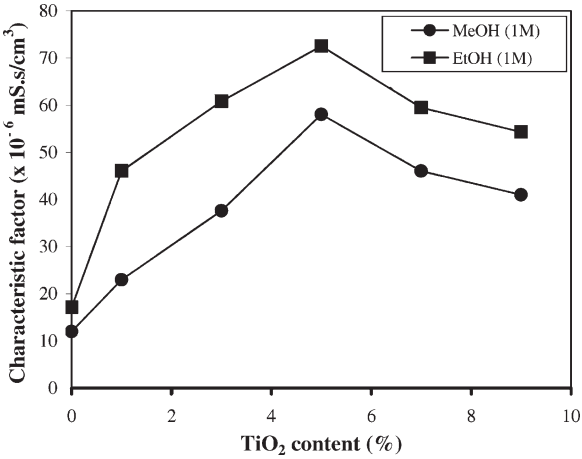

Figure 11.
Characteristic factors of the membranes.

a DAFC application. The characteristic factor for DEFC is 0.072 $\mu S \cdot s/cm^3$ as compared to 0.058 $\mu S \cdot s/cm^3$ for DMFC. Therefore, the DEFC with 1M ethanol solution feed and 5% TiO_2 composite nafion membrane is a potential fuel cell membrane based on *ex-situ* characterization.

Conclusions

This work was focused on the synthesis of nafion/TiO_2 composite membranes from commercially available nafion dispersion by casting method for direct alcohol fuel cell. The composite membranes were extensively characterized for the possible use of the membrane in direct alcohol fuel cell. The methanol and ethanol permeability was reduced with the composite membrane. The membrane with 5% TiO_2 was found to be the best in terms of the lowest methanol or ethanol permeability and at the same time maximizing the proton conductivity. The permeability of ethanol was lower than methanol. The 5% TiO_2 loading decreases the permeability of the membrane for ethanol and methanol by 71% and 75% respectively. Further increase in TiO_2 loading by 7% and 9% do not show significant improvement in reduction of permeation. It has been found that composite membrane prepared by 5% TiO_2 has the maximum characteristic factor for ethanol and thus may be suitable for the DAFC application.

Acknowledgements: The authors gratefully acknowledge the financial support of the Department of Science and Technology, Government of India for the above project (SR/FTP/ETA-29/2007).

[1] S. Surampudi, S. R. Narayanan, E. Vamos, H. Frank, G. Halpert, A. LaConti, J. Kosek, G. K. Surya Prakash, G. A. Olah, *J. Power Sources* **1994**, *47*, 377.
[2] M. Wang, H. Guo, C. Ma, *J. Fuel Cell Sci. Tech.* **2006**, *3*, 202.
[3] W. J. Zhou, S. Q. Song, W. Z. Li, G. Q. Sun, Q. Xin, S. Kontou, K. Poulianitis, P. Tsiakaras, *Solid State Ionics* **2004**, *175*, 797.
[4] S. Ha, R. Larsen, R. I. Masel, *J. Power Sources* **2005**, *144*, 28.
[5] O. Neto, T. R. R. Vasconcelos, R. W. R. V. Da Silva, M. Linardi, E. V. Spinacé, *J. Appl. Electrochem.* **2005**, *35*(2), 193A.
[6] C. Rice, S. Ha, R. I. Masel, P. Waszczuk, A. Wieckowski, T. Barnard, *J. Power Sources* **2002**, *111*, 83.
[7] A. Difoe, A. Verma, U. K. Saha, *The Icfai Univ. J. Mech. Engg.* **2008**, *1*, 30.
[8] S. Song, W. Zhou, Z. L. Zhenxing, R. Cai, G. Sun, Q. Xin, V. Stergiopoulos, P. Tsiakaras, *Appl. Catal., B* **2005**, *55*, 65.
[9] S. Song, G. Wang, W. Zhou, X. Zhao, G. Sun, Q. Xin, S. Kontou, P. Tsiakaras, *J. Power Sources* **2005**, *140*, 103.
[10] S. L. Douvartzides, F. A. Coutelieris, A. K. Demin, P. E. Tsiakaras, *Int. J. Hydrogen Energy* **2004**, *29*(4), 375.

[11] W. J. Zhou, B. Zhou, W. Z. Li, Z. H. Zhou, S. Q. Song, G. Q. Sun, Q. Xin, S. Douvartzides, M. Goula, P. Tasiakaras, *J. Power Sources* **2004**, *126*, 16.
[12] C. Lamy, S. Rousseau, E. M. Belgsir, C. Coutanceau, J. M. Léger, *Electrochim. Acta* **2004**, *49*, 3901.
[13] A. Verma, A. Sharma, S. Basu, *Ind. Chem. Engr.* **2007**, *49*(4), 330.
[14] S. Aricò, P. Cret'i, P. L. Antonucci, V. Antonucci, *Electrochem. Solid-State Lett.* **1998**, *1*(2), 66.
[15] Lamy, E. M. Belgsir, J. M. Lege'r, *J. Appl. Electrochem.* **2001**, *31*, 799.
[16] E. Antolini, *J. Power Sources* **2007**, *170*, 1.
[17] D. Blasi, V. Baglio, A. Stassi, C. D'Urso, V. Antonucci, A. S. Aricò, *ECS Transactions* **2006**, *3*(1), 1317.
[18] R. Tan, L. M. Carvalho, F. Gomes, A. D. Gomes, *Macromol. Symp.* **2006**, *245–246*, 470.
[19] M. Affoune, A. Yamada, M. Umeda, *J. Power Sources* **2005**, *148*, 9.
[20] R. F. Silva, S. Passerini, A. Pozio, *Electrochim. Acta* **2005**, *50*, 2639.
[21] T. A. Zawodzinski, C. Deroin, S. Radzinski, J. Sherman, V. T. Smith, T. E. Springer, *J. Electrochem. Soc.* **1993**, *140*, 1041.
[22] J. W. Rhim, H. B. Park, C. S. Lee, J. H. Jun, D. S. Kim, Y. M. Lee, *J. Membr. Sci.* **2004**, *238*, 143.
[23] J. P. Shina, B. J. Changa, J. H. Kima, S. B. Lee, D. H. Suhb, *J. Membr. Sci.* **2005**, *251*, 247.
[24] L. Barbora, S. Acharya, S. Kaalva, A. Difoe, A. Verma, *Int. J. of Chem. Sci.* **2007**, *5*(4), 1579.
[25] J. Kim, B. Kim, B. Jung, *J. Membr. Sci.* **2002**, *207*, 129.
[26] N. Miyake, J. S. Wainright, R. F. Savinell, *J. Electrochem. Soc.* **2001**, *148*(8), A898.
[27] V. Baglio, A. D. Blasi, A. S. Aric, V. Antonucci, F. S. Fiory, S. Licoccia, E. Traversa, *J. Electrochem. Soc.* **2005**, *152*(7), A1373.
[28] S. S. Sandhu, R. O. Crowther, J. P. Fellner, *Electrochim. Acta* **2005**, *50*, 3985.
[29] P. Staiti, A. S. Arico, V. Baglio, F. Lufrano, E. Passalacqua, V. Antonucci, *Solid State Ionics* **2001**, *145*, 101.
[30] V. Baglio, A. S. Arico, A. D. Blasi, V. Antonucci, P. L. Antonucci, S. Licoccia, E. Traversa, F. S. Fiory, *Electrochim. Acta* **2005**, *50*, 1241.
[31] M. Watanabe, H. Uchida, Y. Seki, M. Emori, P. Stonehart, *J. Electrochem. Soc.* **1996**, *143*(12), 3847.
[32] M. P. Godino, V. M. Barragán, J. P. G. Villaluenga, C. Ruiz-Bauzá, B. Seoane, *J. Power Sources* **2006**, *160*(1), 181.
[33] T. D. Gierke, G. E. Munn, F. C. Wilson, *J. Polym. Sci.* **1981**, *19*, 1687.
[34] M. Mulder (Ed.), in: "*Basic Principles of membrane Technology*", 2nd ed., Kluwer Academic, Dordrecht 1996.
[35] V. Tricoli, *J. Electrochem. Soc.* **1998**, *145*, 3798.

